Thermochimica Acta 485 (2009) 57–64

Contents lists available at ScienceDirect

Thermochimica Acta

journal homepage: www.elsevier.com/locate/tca

Method of preparation does not affect the miscibility between steroid hormone and polymethacrylate

Chutima Wiranidchapong[a,*], Thomas Rades[b], Poj Kulvanich[c], Ian G. Tucker[b]

[a] Department of Pharmaceutical Technology, Faculty of Pharmacy, Srinakharinwirot University, Ongkharak, Nakhon-Nayok 26120, Thailand
[b] School of Pharmacy, University of Otago, Dunedin 9001, New Zealand
[c] Faculty of Pharmaceutical Sciences, Chulalongkorn University, Bangkok 10330, Thailand

ARTICLE INFO

Article history:
Received 28 June 2008
Received in revised form 9 October 2008
Accepted 9 December 2008
Available online 24 December 2008

Keywords:
Steroid hormone
Polymethacrylate
MTDSC
Melting point depression
Drug–polymer interaction
FTIR

ABSTRACT

Miscibility of 17β-estradiol in Eudragit® RS and norethindrone in Eudragit® RS either physical mixes or solid dispersions was determined by modulated temperature differential scanning calorimetry using three heating programs. Heating program I-E revealed the melting point depression of 17β-estradiol in Eudragit® RS as a function of composition, estimated by the Nishi–Wang equation. Heating program II-E disclosed a single glass transition temperature of the blends lying between those of 17β-estradiol and Eudragit® RS, described by the Kwei equation. Heating program I-N demonstrated the reduction of norethindrone melting point when the concentration of Eudragit® RS increased. The parameters determined by the Nishi–Wang and Kwei fits were consistent with the interactions between blend components. No difference in the miscibility and interactions between blend components was observed in the blends prepared by physical mixes and co-evaporation.

1. Introduction

Thermal analysis has been used to determine miscibility of polymer blends prepared by co-evaporation extensively [1–3]. The criteria indicating the miscibility of polymer blends are melting point depression and a single glass transition temperature (T_g) based on Flory–Huggins theory and principle of Gordon–Taylor equation, respectively [1–7]. This technique has been applied to determine the miscibility of drug in polymer matrix in order to select appropriate drug and polymer for development of controlled release system. For example, the miscibility of 17β-estradiol (E_2) in Eudragit® RS (ERS) solid dispersion could be determined by modulated temperature differential scanning calorimetry (MTDSC). The reduction of E_2 melting point and T_g behavior could be estimated by Nishi–Wang and Kwei equations, respectively [8].

The Nishi–Wang equation has been derived from the Flory–Huggins model:

$$T_m - T_{mb} = \frac{-T_m B V_2 \phi_1^2}{\Delta H_2} \quad (1)$$

where T_m and T_{mb} are melting temperatures of pure crystalline component and the blend, respectively; B is the interaction energy density between blend components; V_2 is the molar volume of the repeating unit of the crystalline component; ϕ_1 is the volume fraction of the amorphous component in the blend; and ΔH_2 is the heat of fusion of the crystalline component per mole of the repeating unit [1,2,4,6–8]. The melting point of crystalline component in the blend described by the Nishi–Wang equation implies an interaction between blend components.

The Kwei equation, a modified version of the Gordon–Taylor equation, has been used to predict the T_g of the blend exhibiting an interaction between blend components:

$$T_g = \frac{w_1 T_{g_1} + K w_2 T_{g_2}}{w_1 + K w_2} + q w_1 w_2; \quad K = \frac{\rho_1 T_{g_1}}{\rho_2 T_{g_2}} \quad (2)$$

where T_{gi}, w_i, and ρ_i are the glass transition temperatures, the weight fractions and the densities of blend components; q is an adjustable parameter corresponding to the strength of hydrogen bonding in the blend [1–3,5]. The original equation, the Gordon–Taylor, predicts the T_g of the blend based on the glass transition temperatures and the weight fractions of blend components as illustrated in following equation [9–11]:

$$T_g = \frac{w_1 T_{g_1} + K w_2 T_{g_2}}{w_1 + K w_2} \quad (3)$$

Most of drugs administered for long-term therapy are of popular to be developed in extended release dosage form in order to increase patient compliance [12–14]. The efficacy of drug treatment depends on the consistency of drug release from such dosage form, having

* Corresponding author. Tel.: +66 2 6641000x1607; fax: +66 37 395096.
E-mail address: chutimav@swu.ac.th (C. Wiranidchapong).

0040-6031/$ – see front matter © 2008 Elsevier B.V. All rights reserved.
doi:10.1016/j.tca.2008.12.013

the uniformity of drug distribution in polymer matrix [15–17]. Miscibility between drug and polymer promotes the uniformity of drug distribution in the polymer matrix [8,18]. However, the miscibility of drug in polymer matrix has rarely been reported.

According to the determination of the miscibility between drug and polymer by MTDSC, solid dispersions of drug in polymer are usually prepared by co-evaporation [1–3,8]. Much organic solvent is necessary to dissolve blend components. Most organic solvents are toxic and harmful to the environment. To avoid the usage of organic solvent, the blend may alternatively be prepared by physical mix before characterized by MTDSC. If physical mix is possible to prepare a blend, cost and time consuming of analysis will decrease. Thus, it is a rationale to utilize this technique as a high throughput screening for suitable drug and polymer in development of extended release dosage form.

The objectives of this study were to investigate the miscibility between ERS and norethindrone (NET), normally administered in combination with E_2 for contraception [15,19], by MTDSC and to determine if methods of preparation, i.e., physical mix and co-evaporation, of blends of E_2 in ERS and NET in ERS affected the miscibility and their specific interactions.

2. Experimental

2.1. Materials

E_2-hemihydrate and NET were purchased from Fluka Chemie GmbH, Buchs, Germany and Sigma–Aldrich, Steinheim, Germany, respectively. ERS (Röhm Pharma GmbH, Germany) was supplied as a gift by JJ Degussa, Thailand. Absolute ethanol was of reagent grade (Merck, Germany).

2.2. Preparation of drug in polymer blends

Blends of E_2 in ERS and NET in ERS were prepared by either physically mix with mortar and pestle for 5 min or absolute ethanol evaporation as previously described [8] using E_2/ERS mass ratios of 1/99–90/10 and NET/ERS mass ratios of 10/90–90/10, respectively. The blends were kept in a desiccator over silica gel at room temperature.

2.3. Thermal analysis

Differential scanning calorimetry (DSC) curve of NET was carried out using a Mettler Toledo DSC apparatus with a refrigerated cooling system (DSC 823e, Switzerland) and nitrogen as purge gas. The DSC cell was calibrated with indium (melting point 156.9 °C and ΔH = 27.5 J/g). NET (≈19.6 mg) was accurately weighed into standard aluminum pan with cover (closed pan) and scanned using the following heating program: heating to 230 °C at 5 K/min; cooling to 0 °C at 5 K/min; heating to 230 °C at 5 K/min.

The melting point depression and T_g behavior of the blends (approximately accurate weight of 4 mg) were investigated by a TA Q100 Modulated DSC with a refrigerated cooling system (TA Instruments, New Castle, DE). The melting points of NET in the blends (NET/ERS mass ratios of 10/99–90/10) and E_2 in the blends (E_2/ERS mass ratios of 20/80–90/10) were determined by heating program I-N and I-E, respectively. The T_g values of the blends (E_2/ERS mass ratios of 1/99–90/10) were determined by heating program II-E. Heating program I-N: heating from 25 to 250 °C at 5 K/min. Heating program I-E: heating from 25 to 120 °C at 10 K/min, cooling to 25 °C at 20 K/min, an isothermal period for 5 min at 25 °C, and finally heating to 250 °C at 5 K/min. Heating program II-E: heating from 25 to 182 °C at 10 K/min, cooling to 25 °C at 20 K/min, an isothermal period for 5 min at 25 °C, and finally heating to 250 °C at 5 K/min. A modulation amplitude of ±1 °C and a period of 60 s were used. The heating program I-E allowed only one polymorphic form of E_2 in the blends to be determined its melting point whereas the heating program II-E enabled amorphous E_2 blended with ERS after the first heating run causing alteration of the T_g of the blends as previously described [8].

2.4. Mathematical analysis

The melting points of E_2 in the blends (E_2/ERS mass ratios of 20/80–90/10) and NET in the blends (NET/ERS mass ratios of 10/99–90/10) determined by MTDSC were fitted to the Nishi–Wang equation. The B value was estimated by non-linear regression analysis (GraphPad Prism® version 4.0). ΔH_2 (143.2 J/g), T_m (179.9 °C), V_2 (167.0 cm^3), and ϕ_1 calculated from the weight fractions and densities of E_2 (1.61 g/cm^3) and ERS (1.10 g/cm^3) [8,20] were used for the fits of the E_2 melting points to the Nishi–Wang equation. For the fits of the NET melting points to the Nishi–Wang equation, ΔH_2 (190.8 J/g), T_m (209.4 °C), V_2 (191.2 cm^3), and ϕ_1 calculated from the weight fractions and densities of NET (1.56 g/cm^3) and ERS were used [20]. Nine experimental data points obtained from both physical mixes and solid dispersions were used for each fit. The coefficient of determination (R^2) and randomness of the residuals were used to determine the goodness of fit.

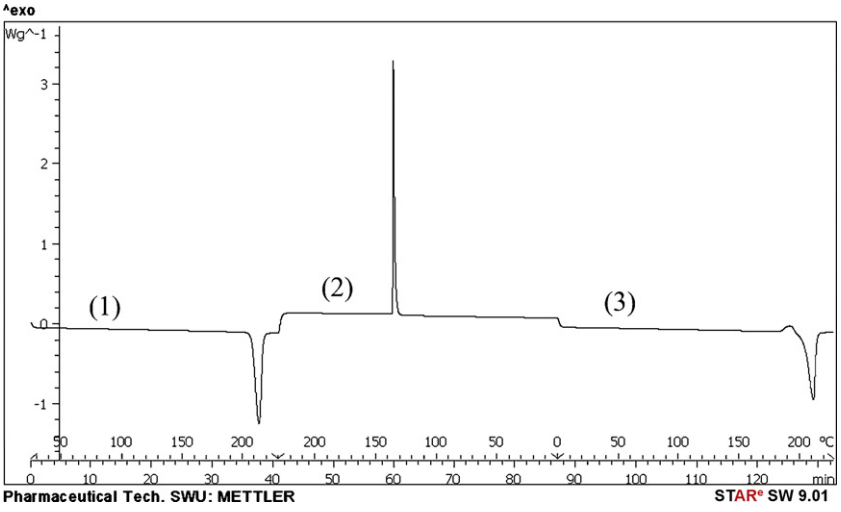

Fig. 1. DSC curve of NET. Program: (1) heating to 230 °C at 5 K/min; (2) cooling to 0 °C at 5 K/min; (3) heating to 230 °C at 5 K/min.

Table 1
Melting points (T_{mb}) and heats of fusion (ΔH) of E_2 in ERS and NET in ERS either physical mixes or solid dispersions for the concentration range of 0–100% (w/w) obtained from the reverse heat flow curves of MTDSC scanning using heating program I-E and I-N, respectively.

% (w/w) Drug in ERS	Physical mixes		Solid dispersions	
	T_{mb} (°C)	ΔH (J/g)	T_{mb} (°C)	ΔH (J/g)
20% E_2	135.1	3.149	132.1	0.08603
30% E_2	143.3	1.796	147.3	1.093
40% E_2	165.1	14.83	153.4	5.184
50% E_2	151.8	6.603	159.6	15.73
60% E_2	172.0	40.27	168.7	28.30
75% E_2	170.4	38.08	172.2	42.05
80% E_2	177.6	71.76	175.1	53.05
90% E_2	179.2	93.88	178.5	129.9
100% E_2	179.9	143.2	179.9	143.2
10% NET	172.9	0.1157	176.6	0.1009
30% NET	178.3	12.62	181.5	8.717
40% NET	184.2	27.23	189.7	27.06
50% NET	192.9	41.00	195.7	43.30
60% NET	198.2	54.16	201.6	52.18
75% NET	205.1	87.75	205.8	86.71
80% NET	204.0	76.82	204.6	57.75
90% NET	206.3	129.7	207.2	45.82
100% NET	209.4	190.8	209.4	190.8

Using non-linear regression analysis, the T_g versus w_1 data from the MTDSC measurements of E_2 in ERS either physical mixes or solid dispersions (0–100%, w/w) were fitted to the Gordon–Taylor and Kwei equations. T_{g1} and T_{g2} were obtained from MTDSC curves of ERS and E_2, respectively. K was estimated from the Gordon–Taylor fit and K and q from the Kwei fit. Thirteen experimental data points were used for each fit. The coefficient of determination (R^2) and the residual plot were used to evaluate the goodness of each fit. The best model was selected on the basis of the Akaike information criterion (AIC) [8,21].

2.5. Fourier transform infrared spectroscopy (FTIR)

FTIR spectra of ERS, E_2, NET and the blends either physical mixes or solid dispersions of E_2 to ERS mass ratios of 20/80, 50/50 and 75/25, not heated and heated from 25 to 175 °C at a heating rate of 5 K/min, and NET to ERS mass ratios of 30/70, 50/50 and 75/25, not heated and heated from 25 to 210 °C at a heating rate of 5 K/min, were performed with a Perkin-Elmer FTIR Spectrum One using potassium bromide disks. Spectrometer adjustments were: resolution of 4 cm^{-1} and sample scan of 64 times.

3. Results and discussion

3.1. DSC curve of NET

It was shown that only one endothermic peak corresponding to melting point of NET was observed at 209.9 °C in the first heating run (DSC; 25–230 °C at 5 K/min). On cooling (DSC; 230–0 °C at 5 K/min) an exothermic peak was observed at 145.4 °C, indicating the transformation of molten NET to crystalline NET. This phenomenon was confirmed by an endothermic peak at 209.9 °C

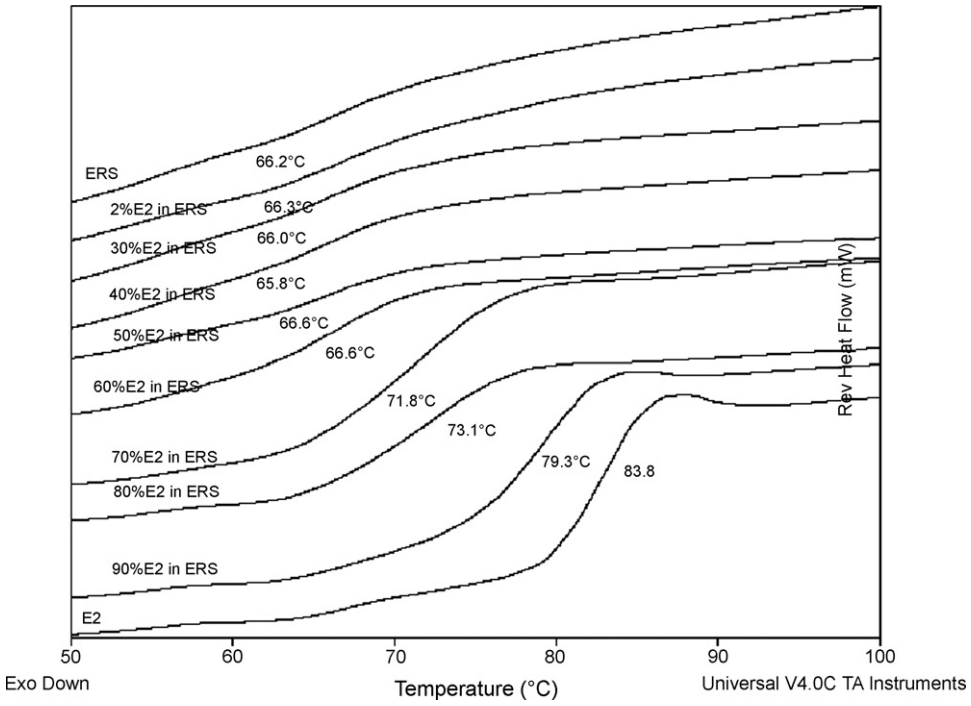

Fig. 2. Reverse heat flow curves of E_2 in ERS physical mixes at concentration range of 0–100% (w/w) obtained from MTDSC scanning using heating program II-E.

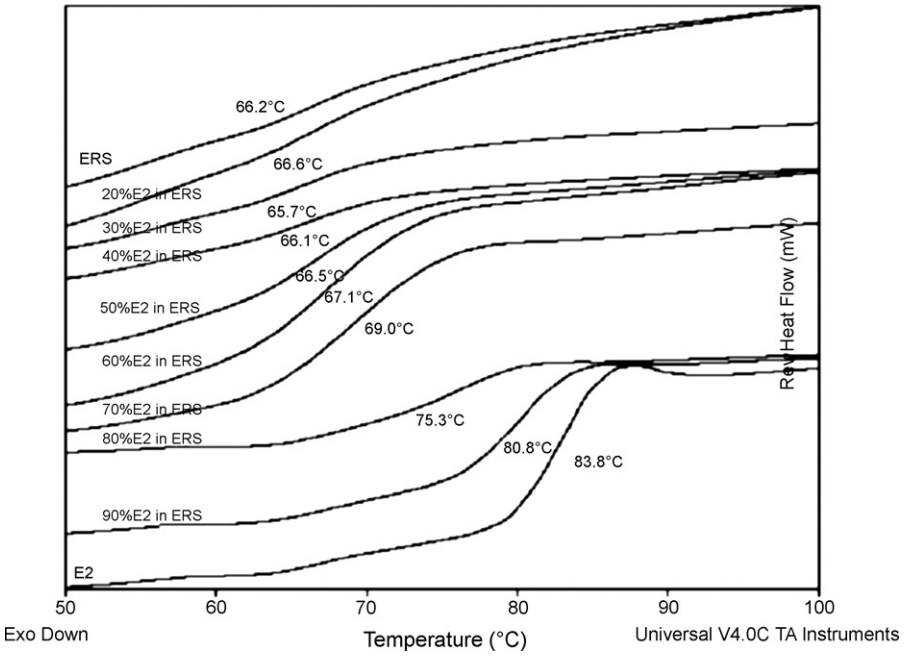

Fig. 3. Reverse heat flow curves of E_2 in ERS solid dispersions at concentration range of 0–100% (w/w) obtained from MTDSC scanning using heating program II-E.

in the second heating run (DSC; 0–230 °C at 5 K/min) as shown in Fig. 1. This suggests that NET is a crystalline form in nature. In determination of the miscibility between NET and ERS in either physical mixes or solid dispersions by thermal analysis, crystalline NET was blended with ERS. Thus, only the melting point depression of NET was used as a criterion according to the Flory–Huggins theory.

3.2. MTDSC analysis of the melting points of E_2 and NET in the blends

The melting points and heats of fusion of E_2, NET and the blends containing E_2 to ERS mass ratios of 20/80–90/10 and NET to ERS mass ratios of 10/90–90/10 either physical mixes or solid dispersions are presented in Table 1. MTDSC analysis using heating program I-E demonstrated the reduction of the melting point and heat of fusion of E_2 when the concentration of ERS increased in both types of the blends. In the same way MTDSC analysis using heating program I-N revealed the reduction of the melting point and heat of fusion of NET in the blends when the concentration of ERS increased. These results indicated the miscibility of E_2 in ERS and NET in ERS in the molten state. The methods of blend preparation, i.e., physical mix and co-evaporation, gave similar outcome of the miscibility when the melting point depression was used as a criterion.

3.3. MTDSC analysis of the T_g of E_2 in ERS in the blends

The T_g values of E_2, ERS, and the blends containing E_2 to ERS mass ratios of 1/90–90/10 in both physical mixes and solid dispersions are illustrated in Figs. 2 and 3, respectively. The T_g of the blends obtained from the second heating run (MTDSC; 25–250 °C, 5 K/min) of heating program II-E exhibited a single T_g lying between those of ERS (66.2 °C) and E_2 (83.8 °C) as a function of composition. The T_g values of E_2 in ERS in either physical mixes or solid dispersions shifted towards the T_g of E_2 as weight fractions of amorphous E_2 increased. This suggests that the method of preparation does not affect the result of the miscibility between E_2 and ERS when using a criterion based on the principle of Gordon–Taylor equation.

3.4. Melting point depression analysis

The melting points of E_2 and NET in the blends either physical mixes or solid dispersions were fitted to the Nishi–Wang equation as shown in Figs. 4–7(a), respectively. Good agreement between predicted T_{mb} and experimental T_{mb}, with randomness of residuals and R^2 of 0.8737 and 0.9804 were observed for the fits of E_2 melting points to the Nishi–Wang of physical mixes and solid dispersions, respectively. This indicated validity of the Nishi–Wang equation to predict the E_2 melting points, miscibility and specific interaction between E_2 and ERS in molten state in both types of the blends. The B values obtained from curve fitting of physical mixes and

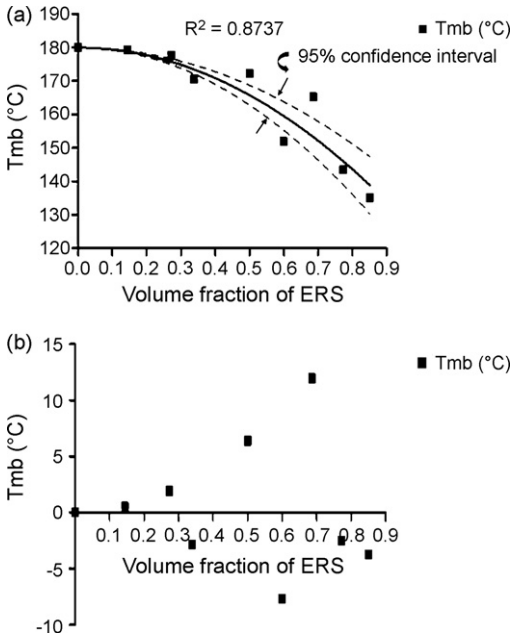

Fig. 4. (a) Fit of experimental data to Nishi–Wang equation: T_{mb} of E_2 in ERS physical mixes obtained from (■) experimental data; (–) predicted by Nishi–Wang equation. (b) Residuals analysis corresponding to the fit.

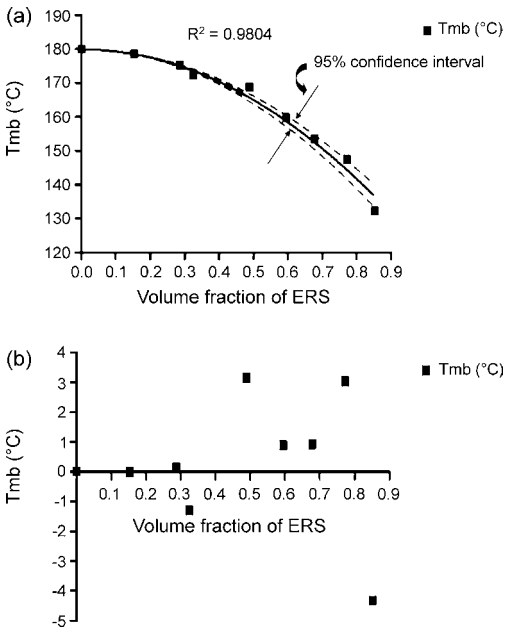

Fig. 5. (a) Fit of experimental data to Nishi–Wang equation: T_{mb} of E_2 in ERS solid dispersions obtained from (■) experimental data; (–) predicted by Nishi–Wang equation. (b) Residuals analysis corresponding to the fit.

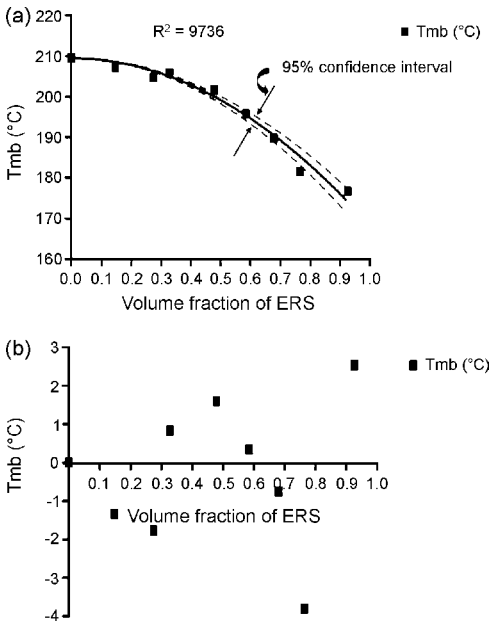

Fig. 7. (a) Fit of experimental data to Nishi–Wang equation: T_{mb} of NET in ERS solid dispersions obtained from (■) experimental data; (–) predicted by Nishi–Wang equation. (b) Residuals analysis corresponding to the fit.

solid dispersions were -0.27 ± 0.024 and $-0.28 \pm 0.0094\,J/(g\,cm^3)$, respectively.

The fits of NET melting points in physical mixes and solid dispersions to the Nishi–Wang gave R^2 of 0.9644 and 0.9736, respectively. The B values obtained from curve fitting of physical mixes and solid dispersions were $-0.23 \pm 0.0098)$ and $-0.20 \pm 0.0075\,J/(g\,cm^3)$, respectively. The residuals corresponding to both fits were apparently non-random. Thus, although both fits give good agreement between predicted T_{mb} and experimental T_{mb}, the non-randomness of the residuals suggests that even this model does not explain the data completely.

3.5. T_g analysis

The T_g values of E_2 in ERS in both physical mixes and solid dispersions were fitted to the Gordon–Taylor equation and its modified version, the Kwei equation as presented in Fig. 8. R^2 obtained from fitting experimental T_g of physical mixes to the Gordon–Taylor and Kwei equations were 0.9286 and 0.9804, respectively. For solid dispersions R^2 values of the Gordon–Taylor and Kwei fits were 0.8932 and 0.9500, respectively. The AIC was used to choose the better model, with the lower values for the AIC indicating the better model. For physical mixes the AIC for the Gordon–Taylor and Kwei fits

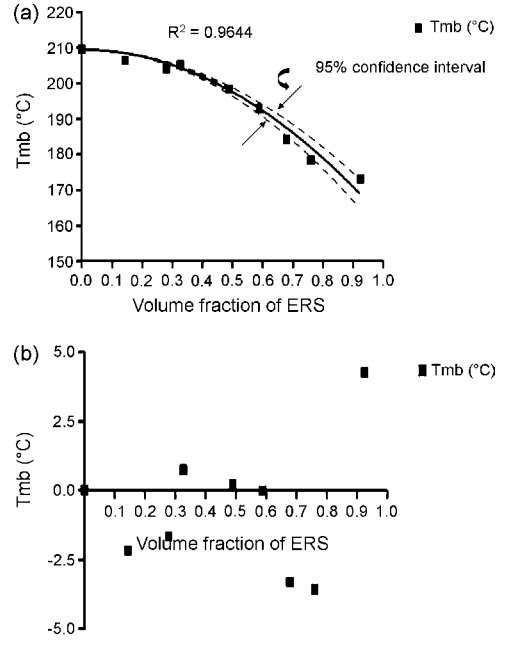

Fig. 6. (a) Fit of experimental data to Nishi–Wang equation: T_{mb} of NET in ERS physical mixes obtained from (■) experimental data; (–) predicted by Nishi–Wang equation. (b) Residuals analysis corresponding to the fit.

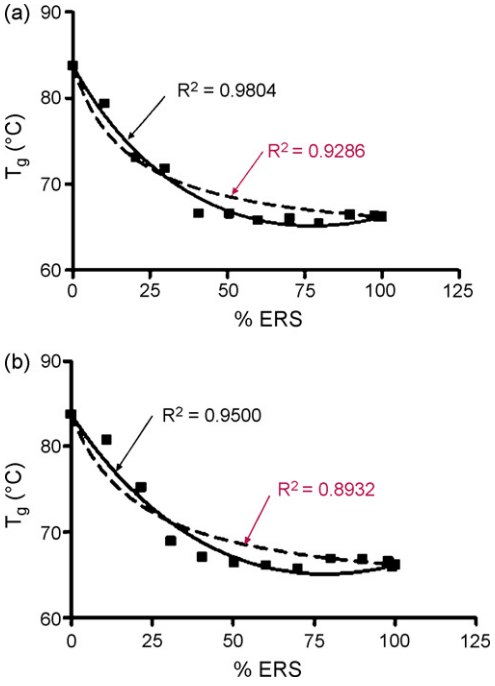

Fig. 8. T_g versus weight fraction of ERS curves based on (■) experimental data; (- - -) Gordon–Taylor equation; (–) Kwei equation. (a) physical mixes; (b) solid dispersions.

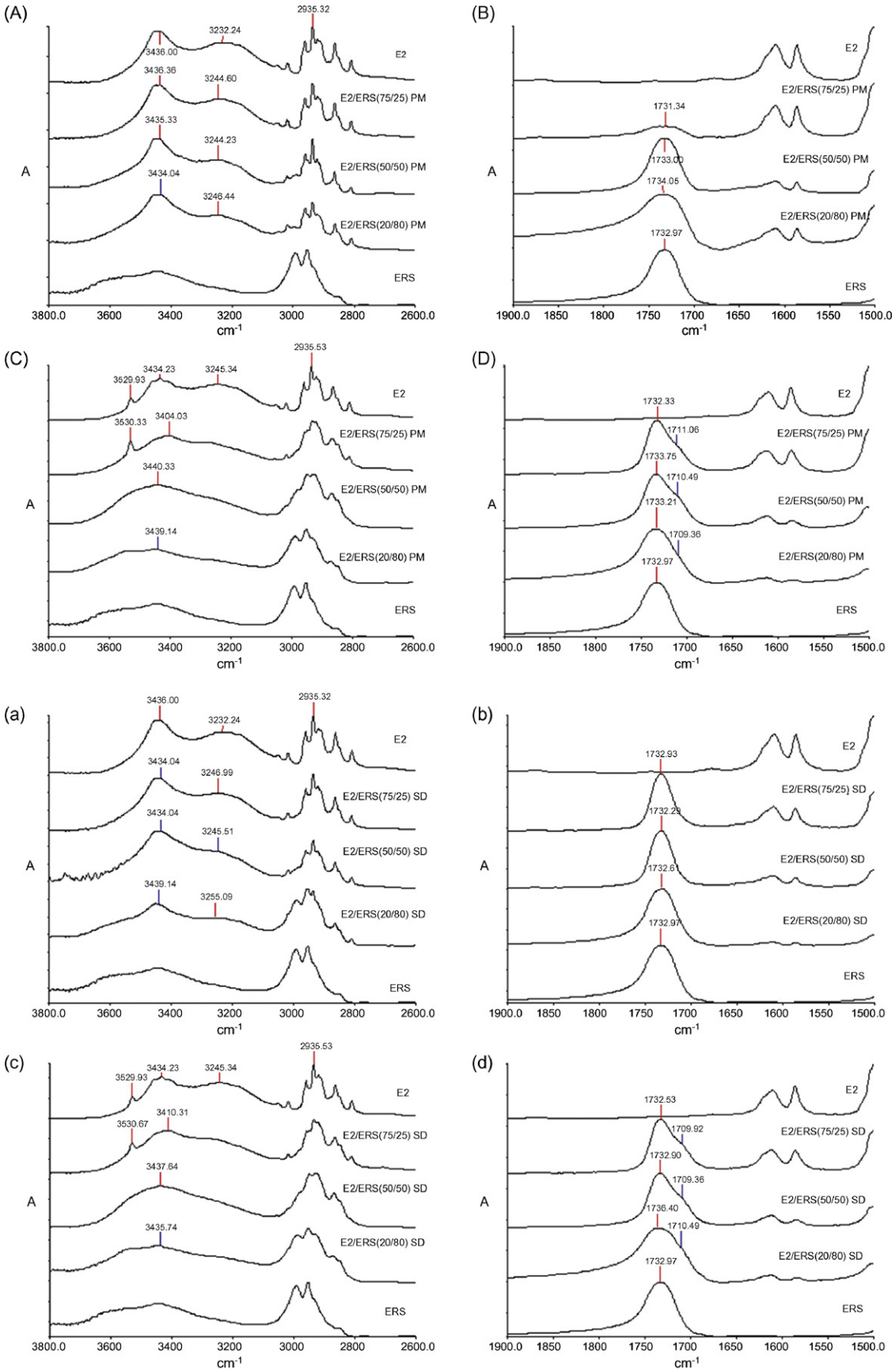

Fig. 9. FTIR spectra of E_2 in ERS physical mixes at a concentration range of 0–100% (w/w), recorded at room temperature in the range of (A) 3800–2600 cm^{-1}; (B) 1900–1500 cm^{-1} and heated from 25 to 175 °C at 5 K/min in the range of (C) 3800–2600 cm^{-1}; (D) 1900–1500 cm^{-1}, and the respective solid dispersions, recorded at room temperature in the range of (a) 3800–2600 cm^{-1}; (b) 1900–1500 cm^{-1} and heated from 25 to 175 °C at 5 K/min in the range of (c) 3800–2600 cm^{-1}; (d) 1900–1500 cm^{-1}.

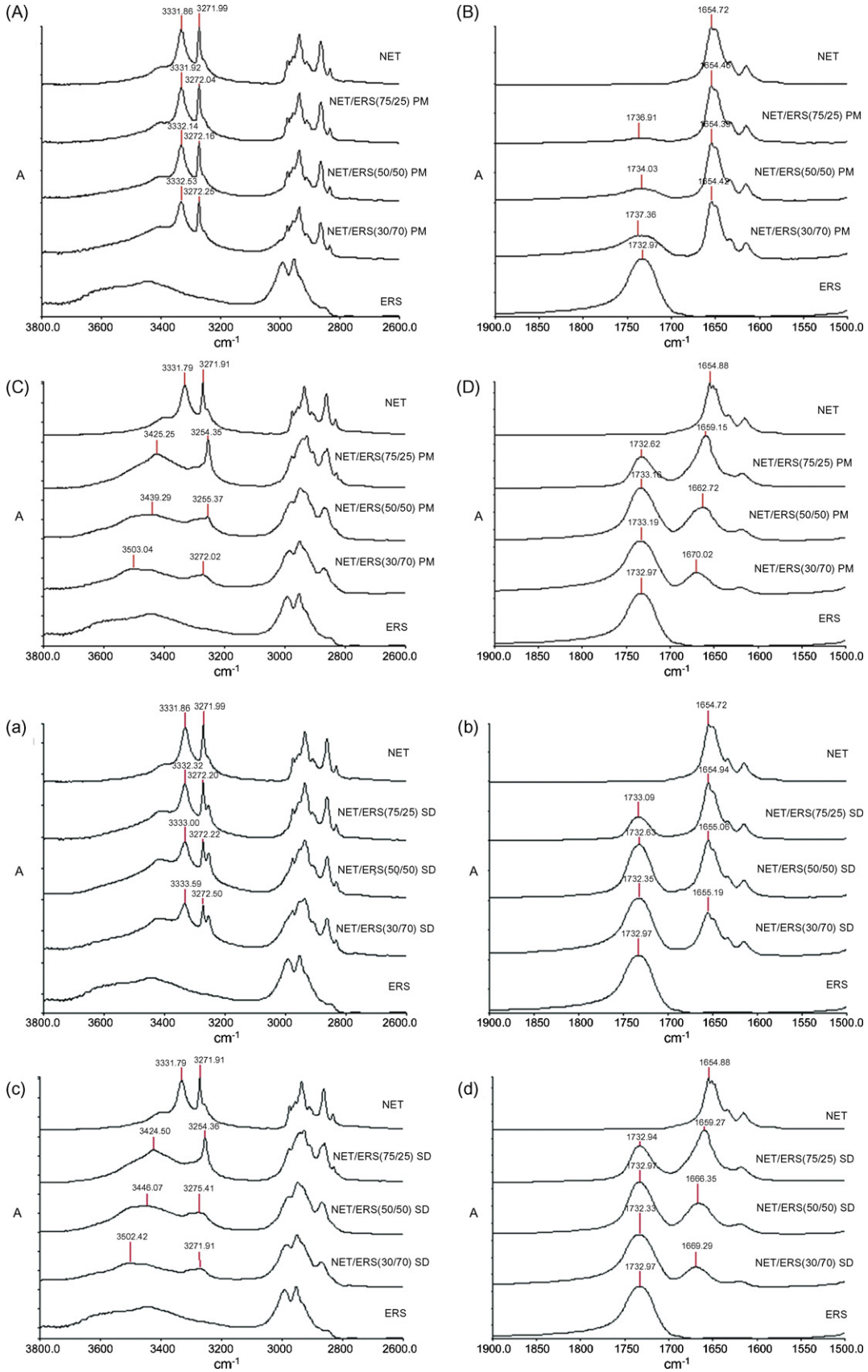

Fig. 10. FTIR spectra of NET in ERS physical mixes at a concentration range of 0–100% (w/w), recorded at room temperature in the range of (A) 3800–2600 cm^{-1}; (B) 1900–1500 cm^{-1} and heated from 25 to 210 °C at 5 K/min in the range of (C) 3800–2600 cm^{-1}; (D) 1900–1500 cm^{-1}, and the respective solid dispersions, recorded at room temperature in the range of (a) 3800–2600 cm^{-1}; (b) 1900–1500 cm^{-1} and heated from 25 to 210 °C at 5 K/min in the range of (c) 3800–2600 cm^{-1}; (d) 1900–1500 cm^{-1}.

were 12.8 and −2.00, respectively. The AIC values of 19.0 and 11.1 were respectively obtained from the Gordon–Taylor and Kwei fits for solid dispersions. Thus, Kwei equation gives a better fit for both kinds of the blends.

For physical mixes K and q values, the Kwei equation parameters, determined by the curve fitting were 0.35 ± 0.084 and -0.0015 ± 0.00039, respectively. For solid dispersions the curve fitting gave K and q values of 0.43 ± 0.21 and -0.0017 ± 0.00081, respectively. The q value is a parameter corresponding to the strength of hydrogen bonding, reflecting the balance between breaking the self-associated hydrogen bonding and formation of inter-associated hydrogen bonding ((1)–(3)). The negative q values obtained from the curve fitting of both physical mixes and solid dispersions indicated that the inter-associated hydrogen bonding between E_2 and ERS was weaker than the self-associated hydrogen bonding of E_2. Both estimated parameters, q and B values determined by the Kwei and Nishi–Wang fits, respectively, indicated the interaction between E_2 and ERS in both physical mixes and solid dispersions.

3.6. FTIR analysis of E_2 in ERS and NET in ERS in the blends

FTIR spectra of E_2 in ERS either physical mixes or solid dispersions showed broad peaks at 3436 and 3232 cm^{-1} attributed to OH stretching of hydroxyl groups adjacent to the C-17 and C-3 positions of E_2, respectively [8,22] and the peak at 1732 cm^{-1} corresponding to the ester C=O stretching vibration of ERS [8,23,24] as presented in Fig. 9. The peak at 1732 cm^{-1} did not change in the blends, not heated to 175 °C at 5 K/min. In both kinds of the blends, heated to 175 °C at 5 K/min, water in the E_2 crystal was removed and the peak around 3530 cm^{-1} corresponding to free hydroxyl group absorption [8,25] was observed in E_2 and E_2 to ERS mass ratio of 75/25. Additionally, the broad peak centered at 3434 cm^{-1} shifted to lower wave number with a shoulder of the ester C=O stretching band around 1710 cm^{-1}, corresponding to the hydrogen-bonded carbonyl group [23,24,26]. For FTIR spectra of E_2 to ERS mass ratios of 50/50 and 20/80 in both types of the blends, heated to 175 °C at 5 K/min, the peak around 3530 cm^{-1} disappeared and broad peaks centered around 3441 and 3437 cm^{-1} were observed with the shoulder of the ester C=O stretching band around 1710 cm^{-1}. This suggested the inter-associated hydrogen bonding between the hydroxyl group of E_2 and the ester C=O group of ERS when water was removed from the E_2 crystal in both kinds of the blends. This phenomenon was in agreement with the negative q and B values, determined by the Kwei and Nishi–Wang fits, respectively, confirming the occurrence of an interaction between E_2 and ERS in molten state in either physical mixes or solid dispersions.

Pure NET demonstrated a sharp peak at 3332 cm^{-1} and a band centered at 1655 cm^{-1} attributed to O–H stretching of free hydroxyl group adjacent to C-17 position and C=O stretching of ketone (C-3 position) conjugated with an alkene, respectively [27,28] (Fig. 10). These two peaks were observed in FTIR spectra of NET to ERS mass ratios of 30/70, 50/50 and 75/25 either physical mixes or solid dispersions with the ester C=O stretching band of ERS around 1732 cm^{-1}. Nothing is changed among these three peaks in the blends, not heated to 210 °C at 5 K/min. For the blends, heated to 210 °C at 5 K/min, the peak at 3332 cm^{-1} shifted to higher wave number with broader band, corresponding to N–H stretching vibration. This suggests a weak bonding between hydroxyl group of NET and amine group of ERS. Additionally, the peak at 1655 cm^{-1} also shifted to higher wave number (around 1670 cm^{-1}), suggesting an inductive effect of ammonium ion on the C=O stretching vibration of C-3 position of NET [27]. However, the ester C=O stretching band of ERS did not alter in the blends, heated to 210 °C at 5 K/min. This suggests that the inter-associated hydrogen bonding between the hydroxyl group of NET and the ester C=O group of ERS do not occur in the molten state.

4. Conclusions

In determination of the miscibility between drug and polymer by thermal analysis, solid state of drug blended with polymer is necessary to choose appropriate criteria for analysis. E_2 can exist in crystalline and amorphous forms, so that, either the melting point depression or the variation of a single T_g as a function of composition can be used as criteria. For NET in ERS blends, NET is in crystalline nature blended with ERS. Thus, only the melting point depression can be used to indicate the miscibility between NET and ERS. Additionally, methods of preparation, i.e., physical mix and co-evaporation, do not affect the miscibility and interactions of E_2 in ERS and NET in ERS in both kinds of the blends.

References

[1] S.W. Kuo, F.C. Chang, Macomolecules 34 (2001) 4089–4097.
[2] S.W. Kuo, C.F. Huang, F.C. Chang, J. Polym. Sci. Part B: Polym. Phys. 39 (2001) 1348–1359.
[3] M. Maldonado-Santoyo, C. Ortíz-Estrada, G. Luna-Bárcenas, I.C. Sanchez, L.C. Cesteros, I. Katime, S.M. Nuño-Donlucas, J. Polym. Sci. Part B: Polym. Phys. 42 (2004) 636–645.
[4] T. Nishi, T.T. Wang, Macromolecules (8) (1975) 909–915.
[5] H.A. Schneider, Macromol. Chem. 189 (1988) 1941–1955.
[6] S.D. Rostami, Eur. Polym. J. 36 (2000) 2285–2290.
[7] S. Pimbert, L. Avignon-Poquillon, G. Levesque, Polymer 43 (2002) 3295–3302.
[8] C. Wiranidchapong, I.G. Tucker, T. Rades, P. Kulvanich, J. Pharm. Sci. 97 (11) (2008) 4879–4888.
[9] L. Fukuoka, M. Makita, S. Yamamura, Chem. Pharm. Bull. 37 (1989) 1047–1050.
[10] D.Q.M. Craig, P.G. Royall, V.L. Kett, M.L. Hopton, Int. J. Pharm. 179 (1999) 179–207.
[11] J.E. Patterson, M.B. James, A.H. Forster, R.W. Lancaster, J.M. Butler, T. Rades, Int. J. Pharm. 336 (2007) 22–34.
[12] Y.W. Chien, in: J. Swarbrick (Ed.), Novel Drug Delivery System, Marcel Dekker, New York, 1982, pp. 465–574.
[13] Y.W. Chien, B.E. Cabana, S.E. Mares, in: J. Swarbrick (Ed.), Novel Drug Delivery Systems, Marcel Dekker, New York, 1982, pp. 311–412.
[14] A. Munoz, Maturitas 33 (1999) s39–s47.
[15] H.S. Pentikis, M.E. Mullin, M. Howard, B. Boutouyrie, G. Rhodes, Curr. Ther. Res. 59 (1998) 681–691.
[16] Y. Qiu, N. Chidambaram, K. Flood, J. Control. Release 51 (1998) 123–130.
[17] B.-T. Liu, J.-P. Hsu, Chem. Eng. Sci. 60 (2005) 5803–5808.
[18] D.J. Greenhalgh, A.C. Williams, P. Timmins, P. York, J. Pharm. Sci. 88 (1999) 1182–1190.
[19] E. Stadberg, P. Westlund, B.-M. Landgren, A.-R. Aedo, S.Z. Cekan, L.-A. Mattsson, Maturitas 33 (1999) 59–69.
[20] D.W. VanKrevelen, Properties of Polymers: Their Correlation with Chemical Structure; Their Numerical Estimation and Prediction from Additive Group Contributions, third ed., Elsevier Science Publishers, Amsterdam, 1990.
[21] S.T. Buckland, K.P. Burnham, N.H. Augustin, Biometrics 53 (1997) 603–618.
[22] S.M. Barnett, I.S. Butler, S. Top, G. Jaouen, Vib. Spectrosc. 8 (1995) 263–277.
[23] R. Pignatello, M. Ferro, G. Puglisi, AAPS Pharm. Sci. Technol. 3 (2002) 1–11.
[24] F. Cilurzo, P. Minghetti, A. Casiraghi, L. Tosi, S. Pagani, L. Montanari, Eur. J. Pharm. Biopharm. 60 (2005) 61–66.
[25] N.E. Variankaval, K.I. Jacob, S.M. Dinh, J. Cryst. Growth 217 (2000) 320–331.
[26] Y. He, B. Zhu, Y. Inoue, Prog. Polym. Sci. 29 (2004) 1021–1051.
[27] R.M. Silverstein, G.C. Bassler, T.C. Morrill, Spectrometric Identification of Organic Compounds, fifth ed., John Wiley & Sons, Singapore, 1991.
[28] R. Bursi, M.B. Groen, Eur. J. Med. Chem. 35 (2000) 787–796.